DORIS Satellite Antenna Maps Derived from Long-Term Residuals Time Series

P. Willis[a,b], S.D. Desai[b], W.I. Bertiger[b], B.J. Haines[b], and A. Auriol[c]

[a]*Institut Géographique National, Direction Technique, 2, Avenue Pasteur, BP 68, 94160 Saint-Mandé, France*

[b]*Jet Propulsion Laboratory, California Institute of Technology, 4800 Oak Grove Drive, MS 238-600, Pasadena CA 91109,USA*

[c]*Centre National d'Etudes Spatiales, 18, avenue E. Belin, 31401 Toulouse, France*

ABSTRACT

Recent studies have shown that phase pattern models for the Jason-1 GPS antenna significantly benefit GPS-based precise orbit determination (POD) for the satellite. We have used a similar technique to derive DORIS receiver antenna maps, using all available DORIS tracking data over long time periods (from 1993.0 to 2004.0). We demonstrate that the derived correction models are satellite specific. For a given satellite, year-to-year estimations show clear systematic patterns. Some of these systematic patterns are attributable to the derivative of the multi-path effects in the direction of the satellite velocity. For early SPOT data, the patterns can be explained by an offset in the TAI time tagging (typically 8 μs). In a second step, we have applied the SPOT2 antenna correction models in precise orbit determination and in the positioning of ground beacons. Preliminary results on DORIS/SPOT2 show that application of the DORIS antenna maps lead to a slight improvement of the derived POD and geodetic results (typically less than 5%).

1. Introduction

The GPS geodetic community has long recognized antenna phase-center variability as a potential source of error in high-accuracy positioning applications (e.g., Melbourne, 1990). Driven in large measure by the ever-increasing accuracies afforded by the GPS system, the topic has received considerable attention in recent years. (e.g., Mader and Czopek, 2002; Rothacher, 2001; Schmid and Rothacher, 2003). In the realm of GPS-based precise orbit determination (POD), the Jason-1 mission carries an ambitious goal of 1-cm for radial accuracy (RMS) of the computed orbits. Achievement of this goal demanded careful consideration of the Jason-1 GPS antenna phase center location and its variability.

The phase center variations of the Jason-1 GPS antennas were precisely measured in an anechoic chamber prior to launch. The effective phase center positions, however, can vary significantly depending on the space environment and local multi-path. In recognition of this, Haines et al. (2003a) solved for the 3D position of the mean antenna phase center using data collected on orbit. The estimation is made possible because the trajectory followed by the mean phase center in inertial space departs from the path taken by the satellite's center of gravity (CG), especially when the satellite is yawing. The CG path is governed by the forces (e.g., gravity) underlying the satellite motion, and can be very well determined in a dynamically constrained POD solution. Departures of the Jason-1 antenna phase center—located about 1.4 m from the CG—from this path can be accommodated by solving for the 3D antenna offset in spacecraft coordinates. A similar approach was used to estimate the phase center offset in the TOPEX/Poseidon (T/P) GPS antenna, albeit in the zenith direction only (Bertiger et al. 1994).

In subsequent studies, Haines et al. (2003b, 2004) adopted a significantly different treatment of the Jason-1 GPS phase-center variations. Rather than solving for the mean location of the phase center, they used on-orbit data to develop maps of the phase-center variations (PCV) as a function of elevation and azimuth in the antenna frame. Underpinning the maps is the value, as measured on the ground in the anechoic chamber, of the mean phase-center location. The maps then describe the incremental variation of the phase center for different lines of sight to the GPS spacecraft. Similar procedures have been in place for evaluating data from terrestrial GPS stations (e.g., Hurst and Bar-Sever, 1998).

The characteristics of the Jason-1 GPS antenna maps hint at a high potential for improving Jason-1 orbit accuracy (Haines et al., 2004). The amount of systematic error explained by the maps is significant in relation to the typical post-fit tracking data residual. Equally important, the patterns in the Jason-1 PCV maps are coherent and stable regardless of the spacecraft attitude. This can be understood in the context of both the spacecraft structure and the space environment: the size and orientation of potential multi-path reflectors are fixed in the antenna frame (excepting the solar panel), and—in contrast with ground stations—there is no residual troposphere signal to confound construction of the map.

Following these examples, Luthcke et al. (2003) have independently developed a map for the Jason-1 antenna, and described the benefits to Jason-1 POD. They observe a general improvement in the Jason-1 radial orbit accuracy over all attitude regimes, but a conspicuous reduction in orbit errors when the satellite is flying in a fixed-yaw mode. Antenna maps for the twin GRACE spacecraft, as well as the GPS satellites themselves, have also been generated (Haines et al., 2004). The precision of the GRACE orbit also has a critical impact on the scientific objectives of this mission (Tapley et al., 2004).

In the present study, we extend the analysis to the DORIS antenna on Jason-1, and other DORIS satellites including the ENVISAT, TOPEX, and the SPOT series. In particular, we investigate the nature of the DORIS Doppler phase-center variations, and examine the potential for improving the DORIS-derived orbits as well as geodetic positioning of ground tracking stations.

2. Generating long-term DORIS residuals time-series

We have reprocessed all DORIS data available at the CDDIS Data Center though the International DORIS Service (IDS) as described by Tavernier et al. (2002). Table 1 summarizes the DORIS data that were actually used from 1993.0 to 2004.0, showing for each satellite the data period, the total number of days used in this study and the total number of generated DORIS residuals. DORIS data were processed using the Gipsy/Oasis II software, as described by Webb and Zumberge (1995). Data were processed on a day-by-day basis using 30-hour solution arcs to allow possible overlap estimations for consecutive days.

Table 2 displays the estimation strategy used for each specific satellite. In particular, we have used our most recent realization of the DORIS Terrestrial Reference Frame (IGN03D02, Willis et al., 2004b) to which we have added more recent DORIS data (through April 2004) for improved velocity determination. Stations coordinates were held fixed in all daily POD solutions. We note that the IGN03D02 reference frame was aligned to ITRF2000 (Altamimi et al., 2002). We have chosen the internal (IGN03D02) reference frame instead of directly using ITRF2000, because the latter would have to be complemented with new stations. Small station-coordinate errors resulting from this process could have significant effects on satellite orbits depending on the station location (Morel and Willis, 2002).

We have used the recent GRACE-derived gravity field GGM01C (Tapley et al., 2004). Willis and Heflin (2004) demonstrated that the use of GGM01C enables significant improvement in the geodetic positioning results of DORIS ground beacons.

In the case of the Jason-1 satellite, the problem created by the anomalous behavior of the on-board clock when crossing the South Atlantic Anomaly (SAA) (Willis et al., 2003; 2004a) was solved by excluding DORIS data for stations inside or closely located to this region of the world. At this writing, this physical phenomenon primarily affects the geodetic results (Willis et al., 2004a). Although the amplitude of the effect is growing almost linearly in time, the POD results have not yet been significantly affected (Luthcke et al., 2003). The DORIS residuals generated for POD estimation from these tracking stations are still meaningful, and precise orbits for the Jason-1 satellite using DORIS data can still be obtained without jeopardizing the scientific altimetry products (Menard et al., 2003, Luthcke et al., 2003). Other approaches for dealing with the SAA effect, like estimating additional parameters, were also recently proposed by Ries (2004). In parallel, other studies have demonstrated the possibility of elaborating a correction model, using simultaneously TOPEX/DORIS and Jason/DORIS data (Lemoine and Capdeville, 2004)

For the Jason-1 satellite we have used the quaternion attitude information when available, and the available attitude model when quaternion data are not available. For TOPEX/Poseidon we have always used the attitude model. For all of the other DORIS satellites we use the Doppler corrections provide by CNES in the original DORIS data files that account for the receiver and transmitter offsets of the center of phase with respect to the reference point.

DORIS data were processed independently for POD on a satellite-by-satellite basis. Such computations can be rather time consuming as it usually takes about 10 hours to process a complete yearly data set for one satellite. The generation of all DORIS residuals from the complete data set available at CDDIS required 5 days with 3 Linux machines used in parallel.

For this study, we have rejected a few days of data when the number of measurements per day was too small (typically when the data represents less than 50% of the average value). The total number of days used is given in Table 1.

3. DORIS antenna maps generation and interpretation

3.1 Going from DORIS residuals to antenna maps

The DORIS antenna PCV maps are defined as functions of azimuth and elevation in the antenna frame. In practice, the PCV maps are numerically implemented by defining nodes at discrete intervals of azimuth and elevation. The phase center correction at any azimuth and elevation is then computed from the bilinear interpolation of the corrections at the four surrounding nodes of the PCV map. The use of bilinear interpolation implies that all of the nodes of the PCV map are correlated with each other to some extent. As such, the phase center corrections at all of the nodes that define the PCV map are simultaneously determined using least squares estimation from all of the post-fit residuals that are available from a specific period of interest. The least squares estimation strategy includes an iterative 3-sigma outlier detection scheme to edit any outliers. The DORIS antenna PCV maps are generated from post-fit residuals that are generated from DORIS-only precise orbit determination (POD) solutions. The daily POD orbit arcs are 30 hours in duration and centered at noon of each day, but only the central 24 hours of post-fit residuals, from 00:00 to 23:59 of each day, are applied to the determination of the PCV maps. This ensures that data are not used twice when generating the maps. Here, one year of post-fit residuals are used to generate each independent PCV map and the nodes of the PCV map are defined at 5-degree intervals in azimuth and elevation.

3.2 DORIS antenna maps interpretation for a satellite

In the case of the DORIS measurement, the residuals correspond to a difference in time (over a time interval of 7 to 10s) of the phase (range) measurement. Fortunately, in the case of the satellite map, the satellite velocity (7 km/s) is much larger than the Earth rotation velocity (0.5 km/s). The pixel that is populated by a single measurement from one station at time t and the pixel that is populated by the subsequent measurement from the same station at time t + Δt are easily related to one another: a line drawn between these two pixels will be oriented nearly parallel to the satellite velocity vector (0–180 azimuth line) when the satellite is not yawing. This implies that the correction can be readily computed from the known Doppler count interval (7–10 s). If GPS satellite antenna maps can be related to possible multi-path on-board the satellite (Haines et al., 2004), then the DORIS satellite maps are the derivatives of the multi-path in the direction of the velocity. This allowed us to directly use the DORIS Doppler antenna map instead of estimating the difference of the antenna map between the 2 corresponding pixels (t and t + Δt). So we have directly computed antenna maps corrections for the Doppler measurements (derivative with time) instead of the DORIS phases and then differentiating these phase corrections with time.

In the case of a DORIS transmitter map (ground station) this property would not be fulfilled anymore and we would have to assess the pixel corresponding to the start of the Doppler count (t) and the pixel corresponding to the end of the Doppler count (t + Δt). We would then have to compute the correction at those 2 different epochs instead of applying the differential correction at the start of the Doppler count only. So we could not use Doppler maps correction anymore but we would really have to develop a more sophisticated algorithm to derive DORIS phase maps. In this study, only satellite (receiver) antenna maps were derived but, as discussed above, this method could also be extended for ground station (transmitter) antenna map corrections.

It must also be noted that the DORIS residuals have always a zero mean per station pass as the estimation of a constant ground clock drift per pass will get rid of all constant term in the residuals (per pass). However, as we will see, taking sub-groups of individual residuals using specific criteria does not imply that the mean is still zero.

3.3 What goes into an individual pixel of the satellite antenna map

The current approach is quite different from the analysis proposed by Doornbos and Willis (2004) wherein DORIS residuals are expressed as a function of the satellite position in the Terrestrial Reference Frame. Such an approach is better suited for detecting systematic effects related to the tracking ground station.

More than 2000 residuals are typically available within each 5 degree by 5-degree pixel of our satellite antenna map models. We have carefully checked that these residuals really depend on the satellite orientation in space only (azimuth and elevation toward the ground station with regards to the satellite frame). In particular, we have verified that in each considered pixel, several ground stations contribute in a random manner. For residuals within the same pixel, the satellite position above the Earth is also evenly distributed on the satellite track. So the signal given in the map has nothing to do with a potential station-dependent effect or any geographically correlated errors coming for example from gravity field errors as discussed by Rosborough and Tapley (1987), and Schrama (1992) and more specifically in the case of TOPEX/Poseidon by Christensen et al. (1994). Furthermore, for each pixel, the day of year of the actual observation is also well distributed so the signal cannot be attributed to an un-modeled seasonal effect.

There are no data corresponding to elevations lower than 27 degrees for SPOT (830 km altitude) and 34 degrees for TOPEX and Jason-1 (1330 km altitude).

4. DORIS antenna maps inter-comparisons

4.1 Time evolution of DORIS antenna maps

Figures 1 to 18 provide examples of these maps derived for all satellites using the GMT software (Wessel and Smith, 1995) for plotting. In particular, Figures 1 to 6 show DORIS antenna maps for the SPOT2 satellites at different epochs. Plots are given in the receiver antenna frame: zero elevation corresponds to the local horizon and 90 degrees elevation is along the antenna boresight (nadir pointing). Zero azimuth corresponds to the spacecraft body-fixed X axis, which is aligned with the velocity vector when the spacecraft is in fixed-yaw mode. In this frame, even if the satellite were yawing, the multipath would not cancel on average but would remain the same if the transmitter remains in the same direction toward the receiver antenna on-board. The effect that we measure is really due to the orientation of the on-board antenna towards the transmitters on-ground rather than the orientation of the spacecraft in space.

These maps derived from independent data sets exhibit a high level of correlation for consecutive years and a limited evolution with time during more than 10 years of observations. Such a conclusion can also be obtained for all other DORIS satellites.

For all satellites, except ENVISAT, DORIS antenna maps can be generated for all azimuth and elevation above the minimum elevation discussed previously. In the case of ENVISAT some data seem to be missing at low elevations when looking backward or forward. This could result from additional masks onboard the satellite due to the configuration of the ENVISAT satellite itself or from some specific preprocessing editing performed by CNES before distributing the data to the IDS.

From all these maps, the SPOT4/1998 map is the most conspicuous outlier (Figure 8), showing a much larger magnitude for the estimated corrections. This behavior is consistent with the problem detected in the early SPOT4/1998 data (Willis and Crétaux, 2004) for which a specific investigation was proposed and will be conducted soon. In the SPOT4/1998 antenna map there is also an asymmetry between the right and the left part of the figure that could be related to a possible error in the cross-track component instead of in the along-track component as discussed below for the other satellites.

4.2 Comparisons of DORIS antenna maps from different satellites

As shown in Figures 1 to 18, DORIS antenna maps are also satellite specific. Satellites such as TOPEX/Poseidon and Jason-1 show very small signal signature, while SPOT and ENVISAT satellites show a larger signal. Table 3 summarizes the magnitude and location of the main signal detected for each satellite.

The SPOT satellites show some similarities in particular, there is a strong negative value in the direction of the back of the satellite. It can also be seen that the early data for the SPOT satellite show a clear, strong signal (negative when looking backwards and positive when looking forward in the direction of the satellite velocity). This signal slowly disappears with time. We will now show that this additional signal can be interpreted as a time-tag bias.

4.3 Interpretation of early SPOT antenna maps

Let us denote O the origin of the frame, S the satellite (receiver) and G the ground station (transmitter). If we further denote: $\vec{u}$ the unit vectors OS, $\vec{v}$ the unit vector toward the satellite velocity, $\vec{a}$ the unit vector in the direction OG, and r and h the orbit and the Earth radius respectively, we have:

$$OS = r\vec{u} \qquad (1)$$
$$OG = h\vec{a}$$

The distance ρ between the satellite (reception) and the receiver (transmission) can be modeled by:

$$\rho = \sqrt{r^2 + h^2 + 2rh\vec{u}.\vec{a}} \qquad (2)$$

If we neglect the eccentricity of the satellite orbit and also the Earth's rotation, the DORIS Doppler measurement D (t) can be modeled by:

$$D(t) = -f\,\frac{\rho(t+\Delta t) - \rho(\Delta t)}{c\Delta t} = -\frac{f}{c}\frac{\partial\rho}{\partial t} \qquad (3)$$

Let us note T the period of the orbit (in seconds) and θ the mean anomaly, we can obtain:

$$D(t) = -\frac{f}{c}\frac{\partial\rho}{\partial\theta}\frac{\partial\theta}{\partial t} = -\frac{f}{c}\frac{\partial\rho}{\partial\theta}\frac{2\pi}{T} \qquad (4)$$

$$D(t) = -\frac{f}{c}\frac{2\pi}{T}\frac{2rh\vec{u}.\vec{a}}{2\rho} \qquad (5)$$

A small time error would affect the Doppler measurement linearly with the time offset DT with a constant coefficient C such as:

$$C = \frac{\partial D}{\partial t} = \frac{\partial D}{\partial\theta}\frac{\partial\theta}{\partial t} = \frac{\partial D}{\partial\theta}\frac{2\pi}{T} \qquad (6)$$

$$C = \frac{f}{c}\left(\frac{2\pi}{T}\right)^2 \frac{rh \frac{\partial(\vec{u}.\vec{a})}{\partial\theta}}{\rho} = \frac{f}{c}\left(\frac{2\pi}{T}\right)^2 \frac{rh}{\rho}\vec{v}.\vec{a} = \frac{f}{c}\left(\frac{2\pi}{T}\right)^2 \frac{rh}{\rho}\sin(\alpha)$$
(7)

In order to create a DD=0.1 mm/s Doppler effect, we need to have a time offset DT that fulfills:

$$DD = C \cdot DT \tag{8}$$

We can now obtain DT

$$DT = \frac{DD}{C} = DD\left(\frac{T}{2\pi}\right)^2 \frac{c}{f}\frac{\rho}{rh\sin(\alpha)} \tag{9}$$

It can be seen that the effect depends on α. For stations in front of the satellite, and station at the back of the satellite the amplitude of the DORIS Doppler residuals will be the same but the sign will be opposite. If we look now at the same problem seen from the point of view of the receiver on-board the satellite, for pixels with the same elevation but with azimuth of opposite sign (station in front versus station behind the satellite), the correction has the same magnitude but an opposite sign. This would show up as an asymmetric pattern in the antenna map.

In the case of the SPOT satellite, we can obtain an estimate of such a time offset to be

$$DT = \frac{DD}{C} = 0.1\left(\frac{100 \cdot 60}{2\pi}\right)^2 \frac{3 \cdot 10^8}{2 \cdot 10^9}\frac{7.2 \cdot 10^9}{(6.4 \cdot 10^9)(2 \cdot 10^9)} \approx 8\mu s \tag{10}$$

5. Validation tests

In a second step, we have processed DORIS/SPOT2 from January 1, 2004 to April 31, 2004 with and without applying the antenna map to look for possible improvement in the precise orbit determination. The map that was used for correction in 2004 was obtained independently using the 2003 DORIS data (No 2004 data was used to generate the antenna map used for correction). We have chosen SPOT2 because the amplitude of the signal is much larger than for TOPEX or Jason-1 for which we would expect a smaller effect using the correction (see Table 3).

5.1 Validating antenna map for POD

We have first computed precise orbit solutions on a daily basis using the same strategy described before. Residuals were very slightly improved (typically 0.4%) but at least no degradation was detected.

Orbit overlaps were also very slightly improved as displayed in Table 4. In our opinion, this demonstrates that in the case of POD larger errors are still coming from dynamic models (drag, surface forces or even gravity field). In fact the orbit precision derived from the orbit overlap tests is already quite good for SPOT-2 (1.4 cm in radial, 5 cm in cross-track and 15 cm in along-track) taking into account the low altitude of the satellite and the limited amount of daily DORIS data, typically 6000 data points for a single channel receiver over 30 hours. These results are far better than those obtained in real-time on-board the satellite using the DIODE software and limited models as described by Jayles et al. (2004), or even older TOPEX orbits as discussed by Nouel et al. (1994) or Yunck et al. (1994) due to regular improvement in DORIS POD processing and the availability of new models.

5.2 Validating the antenna map for geodetic positioning

We have used the same 2004 data set for precise positioning of ground tracking stations, again with and without the antenna maps. Each day, 24-hours of data was processed in a free-network approach, estimating simultaneously the satellite orbit and the stations positions as described in detail in Willis et al. (2004b). Daily sets of station coordinates were then combined in a least squares sense to obtain weekly station positions for all observing DORIS stations. These weekly free-network solutions were then projected and transformed into a specific reference frame using a standard procedure as described by Blewitt et al. (1992) or Sillard and Boucher (2001).

Table 5 summarizes the results obtained using the IGN03D02 reference frame discussed before or an internal reference frame (positions and velocities) derived using only these 4 months of DORIS data in 2004 with and without the antenna maps corrections.

A small but significant improvement (around 5%) could be found for station positioning for each of these terrestrial reference frames. It is encouraging that the 2004 corrected solutions also agree better with the IGN03D02 solution that was obtained over a long time period (more than 10 years). In our opinion, this indicates that when the satellite antenna effect is not corrected, this generates some random errors that can be smoothed using a long time series, as currently done when generating cumulative TRF solutions for IDS.

The positioning accuracy is also quite promising (2.0 to 2.5 cm) when compared to multi-satellite solutions that currently provide a 1.0 to 1.5 cm internal precision doing the same type of tests as demonstrated by Willis and Heflin (2004).

5.3 Discussing possible future steps

In our opinion, it could be important to implement this type of correction for all DORIS satellites simultaneously based on the maps derived in this study. This could be used to test multi-satellite geodetic positioning for ground stations and to look for possible improvement in the current weekly accuracy.

Furthermore a more sophisticated approach could be derived to obtain DORIS antenna phase correction maps for ground stations. This could be used to calibrate both the satellite (receiver) antenna and the ground (transmitter) antenna in a manner similar to what was done for Jason-1 and GRACE in the case of GPS (Haines et al., 2004).

6. Conclusions

We have derived DORIS satellite antenna pattern correction maps for the 7 DORIS satellites available through IDS using orbit residuals computed on a daily basis over the 1993.0-2004.0 period. Such maps were computed every year for every satellite in an independent manner. A simple physical explanation of such a correction map has been proposed in the case of the satellite (receiver). Early SPOT2 maps show an additional residual signal that could be interpreted as a 8 micro-second timing offset which is compatible with the currently assessed precision of the time tagging of the DORIS measurement performed by CNES. For each satellite, the satellite antenna maps are very consistent with each other. However, as expected, these maps differ from one satellite to another. Fortunately, the altimetry missions TOPEX/Poseidon and Jason-1 show smaller residual signals, and the foreseen correction is probably negligible.

In the case of SPOT-2, we have processed 4 months of recent 2004 DORIS data using the map correction generated from the 2003 data. A very small improvement was observed in daily residuals and daily orbit overlaps. For ground station geodetic positioning, however, a slight improvement was obtained when assessing precision of weekly positioning using in a single-satellite mode.

We also propose some possible continuation of this study using a multi-satellite approach. Calibration of DORIS ground stations antenna maps was also discussed.

Acknowledgments

This research was carried out at the Jet Propulsion Laboratory, California Institute of Technology, under a contract with the National Aeronautics and Space Administration.

REFERENCES

Altamimi, Z., P. Sillard, C. Boucher, ITRF2000, A new release of the International Terrestrial Reference Frame for Earth science applications, *J. Geophys. Res.*, **107**, B10, 2214, 2002.

Bertiger, W. I, et al., GPS precise tracking of TOPEX/Poseidon: Results and implications, *J. Geophys. Res.*, **99**(C12), 24,449–24,464, 1994.

Blewitt, G., M.B. Heflin, F.H. Webb, U.J. Lindqwister, R.P. Malla, Global coordinates with centimeter accuracy in the International Terrestrrial Reference Frame using GPS, *Geophys. Res. Lett.*, **19**(9), 853-856, 1992.

Christensen, E.J., B. Haines, K.C. McColl, R.S. Nerem, Observations of geographically correlated orbit errors for TOPEX/Poseidon using the Glocal Positioning System, *Geophys. Res. Lett.*, **21**(19), 2175-2178, 1994.

Doornbos, E., P. Willis, Analysis of DORIS residuals from multiple satellites and POD centers, IDS Plenary Meeting, Paris France, May 3-4, 2004.

Haines, B., W. Bertiger, S. Desai, D. Kuang, T. Munson, L. Young and P. Willis. Initial orbit determination results for Jason-1: Towards a 1-cm orbit, *J. Inst. Navig.*, **50**(3): 171-179, 2003a.

Haines, B., S. Desai, P. Willis, and W. Bertiger, Precise orbit determination for Jason-1: GPS and the 1-cm challenge, *Geophys. Res. Abst.* 5:12378, 2003b.

Haines, B., Y. Bar-Sever, W. Bertiger, S. Desai, P. Willis, One-centimeter orbit determination for Jason-1: new GPS-based strategies, *Marine Geod*, **27**(1-2), 13-770, 299-318, 2004.

Hurst, K. Y.Bar-Sever, Site specific phase center maps for GPS stations (abstract), *EOS Trans. Suppl.*, **79**(45), F183, 1998.

Jayles, C.,M. Costes, Ten centimeters orbits on-board of a satellite, DORIS-DIODE current status, *Acta Astronaut.*, **54**(5), 315-323, 2004.

Lemoine, J.-M., H. Capdeville, Analysis of DORIS frequency on-board Jason, IDS Plenary Session, Paris, France, May 3-4, 2004.

Luthcke, S., N. Zelensky, D.D. Rowlands, F.G. Lemoine, T.A. Williams, The 1-cm orbit Jason-1 precise orbit determination using GPS, SLR, DORIS and altimeter data, *Marine Geod.*, **26**(3-4), 399-421, 2003.

Mader, G.L., F.M. Czopek, The Block IIA satellite, Calibrating Antenna Phase Centers, *GPS World*, 43-46, May 2002.

Melbourne, W. G., GPS-based geodesy tracking: Technology prospects for the Year 2000. "Geodesy in the Year 2000". National Academy Press. Washington, D. C. 124-176, 1990.

Ménard, Y., L.-L. Fu, P. Escudier, F. Parisot, J. Perbos, P. Vincent, S. Desai, B. Haines, G. Kuntsmann, The Jason-1 mission, *Marine Geod.*, **26**(3-4), 131-146, 2003.

Morel, L., P. Willis, Parameter sensitivity of TOPEX orbit and derived mean sea level to DORIS stations coordinates, *Adv. Space Res.*, **30**(2), 255-263, 2002.

Nouel, F., J.-P. Berthias, M. Deleuze, A. Guitart, P. Laudet, A. Piuzzi, D. Pralines, C. Valorge, C. Dejoie, M.F. Susini, D. Taburiau, Precise CNES orbits for TOPEX/Poseidon, Is reaching 2 cm still a challenge? *J. Geophys. Res.*, **99**(C12), 24405-24419, 1994.

Ries, J.-C., Jason-1 orbit determination with DORIS and SLR, an alternative approach for accommodating the SAA effect, IDS Plenary Session, Paris, 2004.

Rosborough, G.W., B.D. Tapley, radial, transverse and normal satellite positioning perturbation due to geopotential, *Celest. Mech.*, **40**, 409, 1987.

Rothacher, M., Combination of absolute and relative antenna phase center variations, *GPS Solutions*, **4**(4), 55-60, 2001.

Schmid, R., M. Rotchacher. Estimation of elevation-dependent satellite antenna phase center variations of GPS satellites. *J. Geod.*, **77**(7-8), 440-446, 2003.

Schrama, E.J.O., Some remarks on several definitions of geographically correlated orbit errors, Consequences for satellite altimetry, *Manuscr. Geod.*, **17**, 282-294, 1992.

Sillard, P., C. Boucher, A review of algebraic constraints in terrestrial reference frame datum definition, *J. Geod.*, **75**(2), 63-73, 2001.

Tapley, B., S. Bettadpur, M.M. Watkins, C. Reigber, The Gravity Recovery and Climate Experiment, Mission Overview and Early Results, Geophys. Res. Lett., **31**, L09607, doi:10.1029/2004GL019920, 2004.

Tavernier, G., L. Soudarin, K. Larson, C. Noll, J. Ries, P. Willis, Current status of the DORIS Pilot Experiment, *Adv. Space Res.*, **30**(2), 151-156, 2002.

Webb, F., J. Zumberge (Eds), An introduction to Gipsy/Oasis II, *Report*, Jet Propulsion laboratory, Pasadena, USA, JPLM D-11088, 1995.

Wessel, P., Smith, W.H.F. New version of the Generic Mapping Tools released. EOS Trans Amer Geophys U 76, 1995.

Willis, P., J.-P. Crétaux, DORIS data analysis strategies, Position Paper, IDS Plenary meeting, Paris, May 3-4, 2004

Willis, P. M. Heflin, External validation of the GRACE GGM01C gravity field using GPS and DORIS positioning results, *Geophys. Res. Lett.*, 31(13), L13616, doi: 10.1029/2004GL020038, 2004.

Willis, P. B. Haines, Y. Bar-Sever, W. Bertiger, R. Muellerschoen, D. Kuang, S. Desai, TOPEX/Jason combined GPS/DORIS orbit determination in the tandem phase, *Adv. Space Res.*, **31**(8), 1941-1946, 2003.

Willis, P., B. Haines, J.-P. Berthias, P. Sengenes, J.-L. le Mouel, Comportement de l'oscillateur DORIS/Jason au passage de l'anomalie sud-atlantique (Behavior of the

DORIS/Jason oscillator over the South Atlantic Anomaly), *C.R.Geosci.*, **336**(9), 839-846, doi:10.1016/j.crte.2004/01.004, 2004a.

Willis, P., C. Boucher, H. Fagard, Z. Altamimi, Geodetic applications of the DORIS system at the Institut Géographique National, *C.R. Geosci.*, 2004b, in press.

Yunck,. T. P., W.I. Bertiger, S.C. Wu, Y. Bar-Sever, E.J. Christiansen, B.J. Haines, S.M. Lichten, R.J. Muellerschoen, Y. Vigue, P. Willis, First assessment of GPS-based reduced dynamic orbit determination on TOPEX/Poseidon, *Geophys. Res. Lett.*,. **21**(7), 541–544, 1994.

Figures Caption

Figure 1: DORIS SPOT2 antenna map derived from 1995 data

Figure 2: DORIS SPOT2 antenna map derived from 1997 data

Figure 3: DORIS SPOT2 antenna map derived from 1999 data

Figure 4: DORIS SPOT2 antenna map derived from 2001 data

Figure 5: DORIS SPOT2 antenna map derived from 2003 data

Figure 6: DORIS SPOT3 antenna map derived from 1995 data

Figure 7: DORIS SPOT3 antenna map derived from 1996 data

Figure 8: DORIS SPOT4 antenna map derived from 1998 data

Figure 9: DORIS SPOT4 antenna map derived from 2002 data

Figure 10: DORIS SPOT4 antenna map derived from 2003 data

Figure 11: DORIS SPOT5 antenna map derived from 2002 data

Figure 12: DORIS SPOT5 antenna map derived from 2003 data

SPOT2 1995

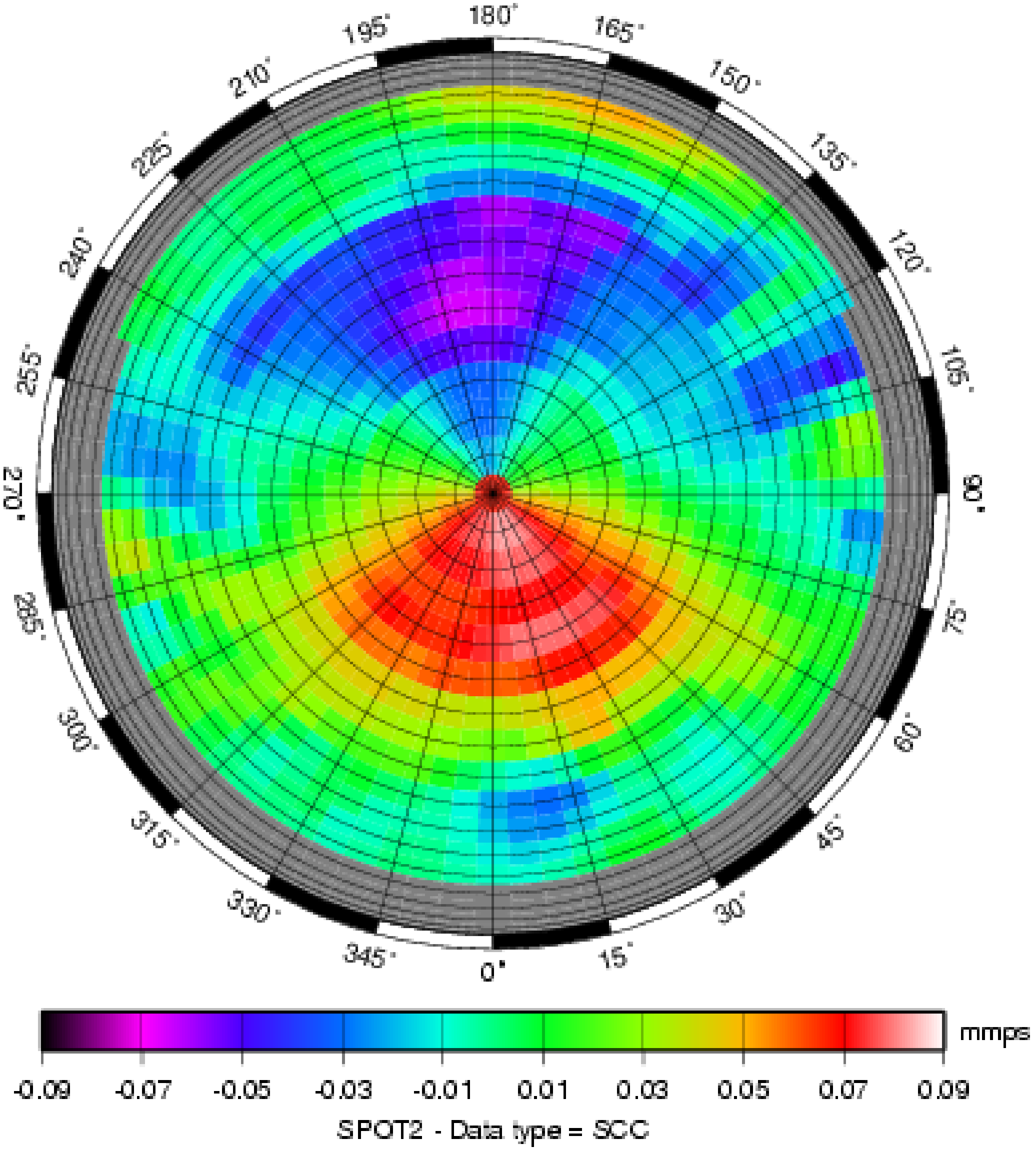

180°
195°
165°
210°
150°
225°
135°
240°
120°
255°
105°
270°
90°
285°
75°
300°
60°
315°
45°
330°
30°
345°
15°
0°
mmps
-0.09
-0.07
-0.05
-0.03
-0.01
0.01
0.03
0.05
0.07
0.09
SPOT2 - Data type = SCC

SPOT2 1997

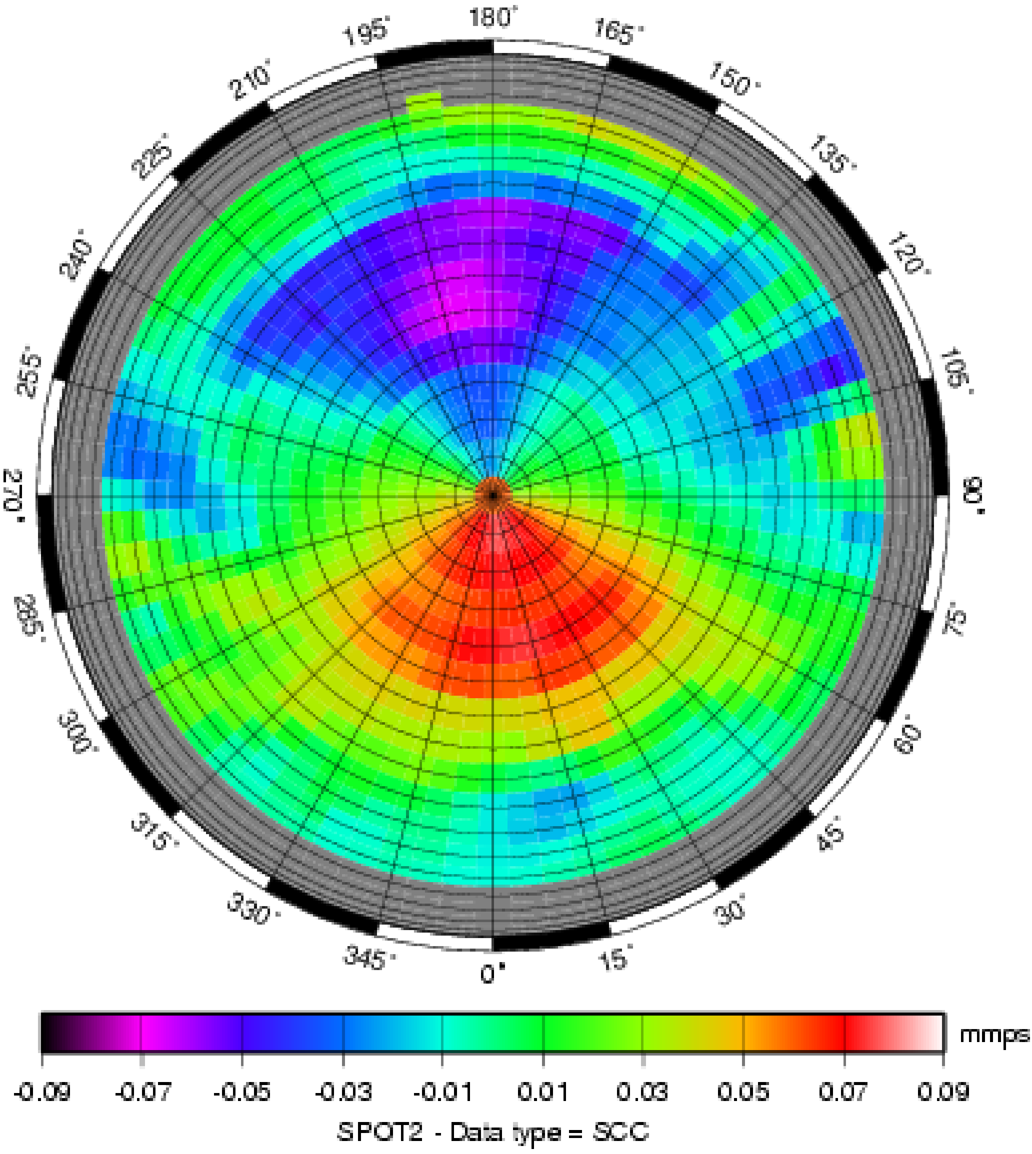

180°
165°
150°
135°
120°
105°
90°
75°
60°
45°
30°
15°
0°
345°
330°
315°
300°
285°
270°
255°
240°
225°
210°
195°
mmps
-0.09
-0.07
-0.05
-0.03
-0.01
0.01
0.03
0.05
0.07
0.09
SPOT2 - Data type = SCC

SPOT2 1999

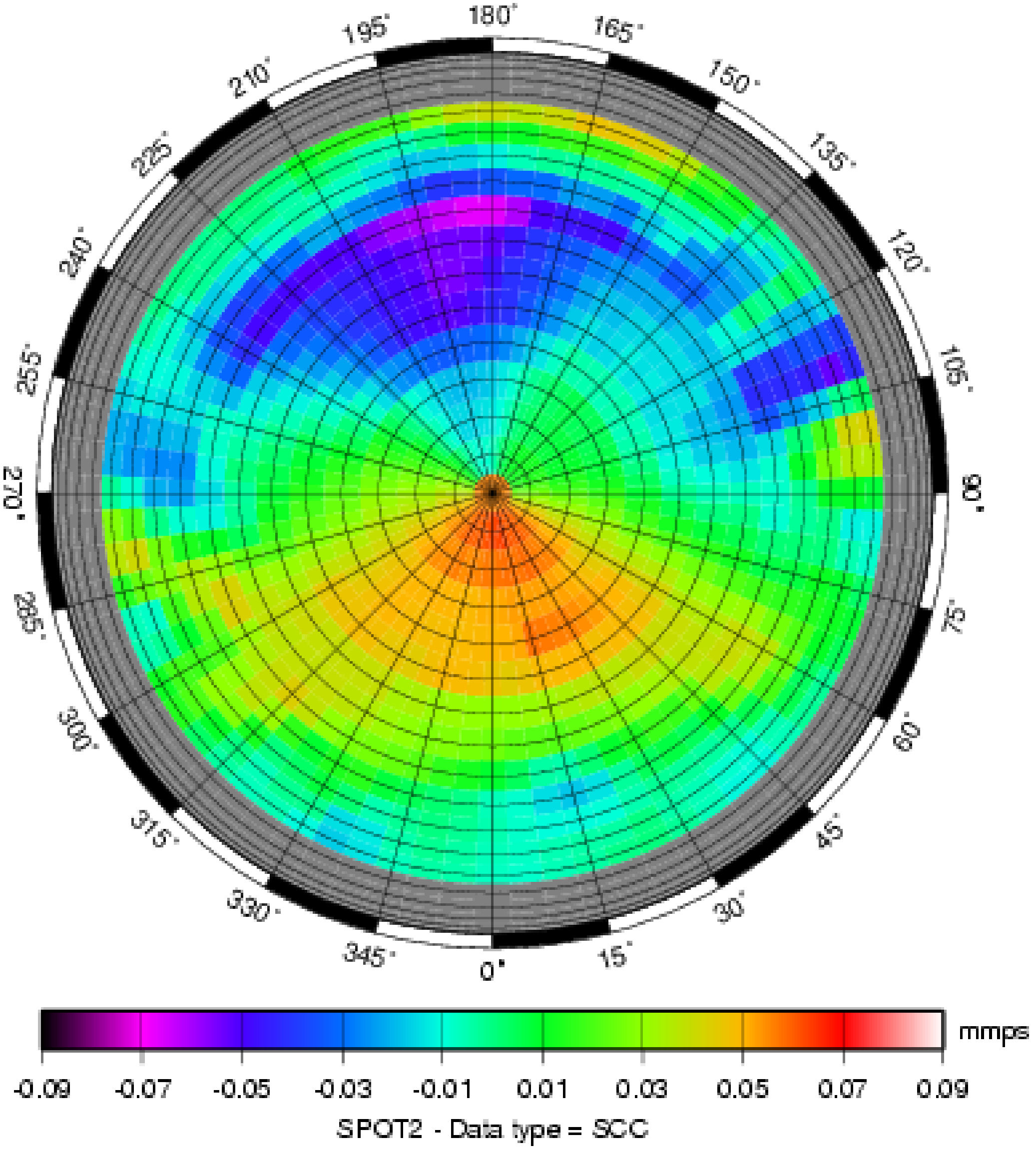

180°
195°
165°
210°
150°
225°
135°
240°
120°
255°
105°
270°
90°
285°
75°
300°
60°
315°
45°
330°
30°
345°
15°
0°
mmps
-0.09
-0.07
-0.05
-0.03
-0.01
0.01
0.03
0.05
0.07
0.09
SPOT2 - Data type = SCC

SPOT2 2001

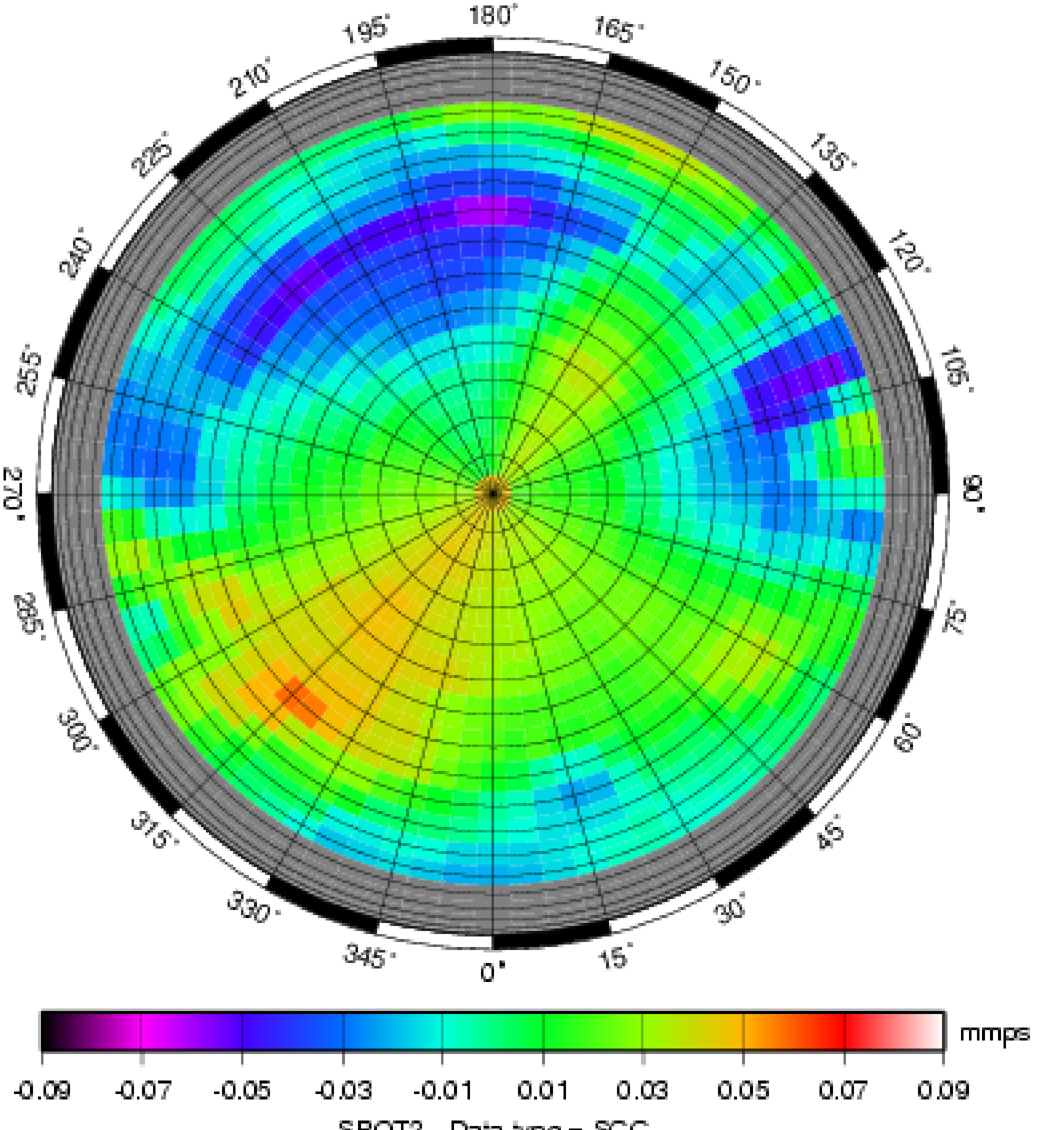

SPOT2 - Data type = SCC

SPOT2 2003

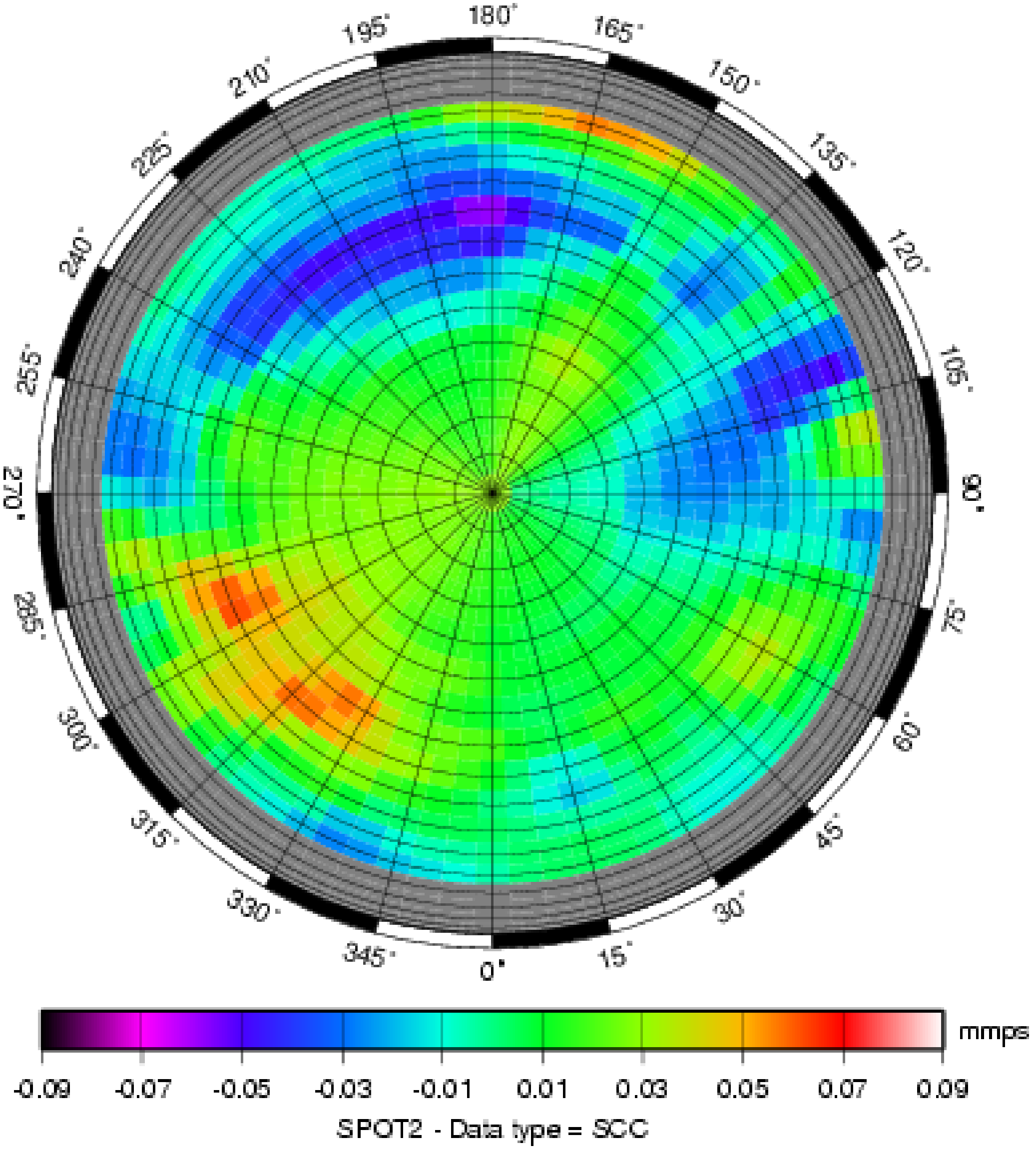
180°
165°
150°
135°
120°
105°
90°
75°
60°
45°
30°
15°
0°
345°
330°
315°
300°
285°
270°
255°
240°
225°
210°
195°
mmps
-0.09
-0.07
-0.05
-0.03
-0.01
0.01
0.03
0.05
0.07
0.09
SPOT2 - Data type = SCC

SPOT3 1995

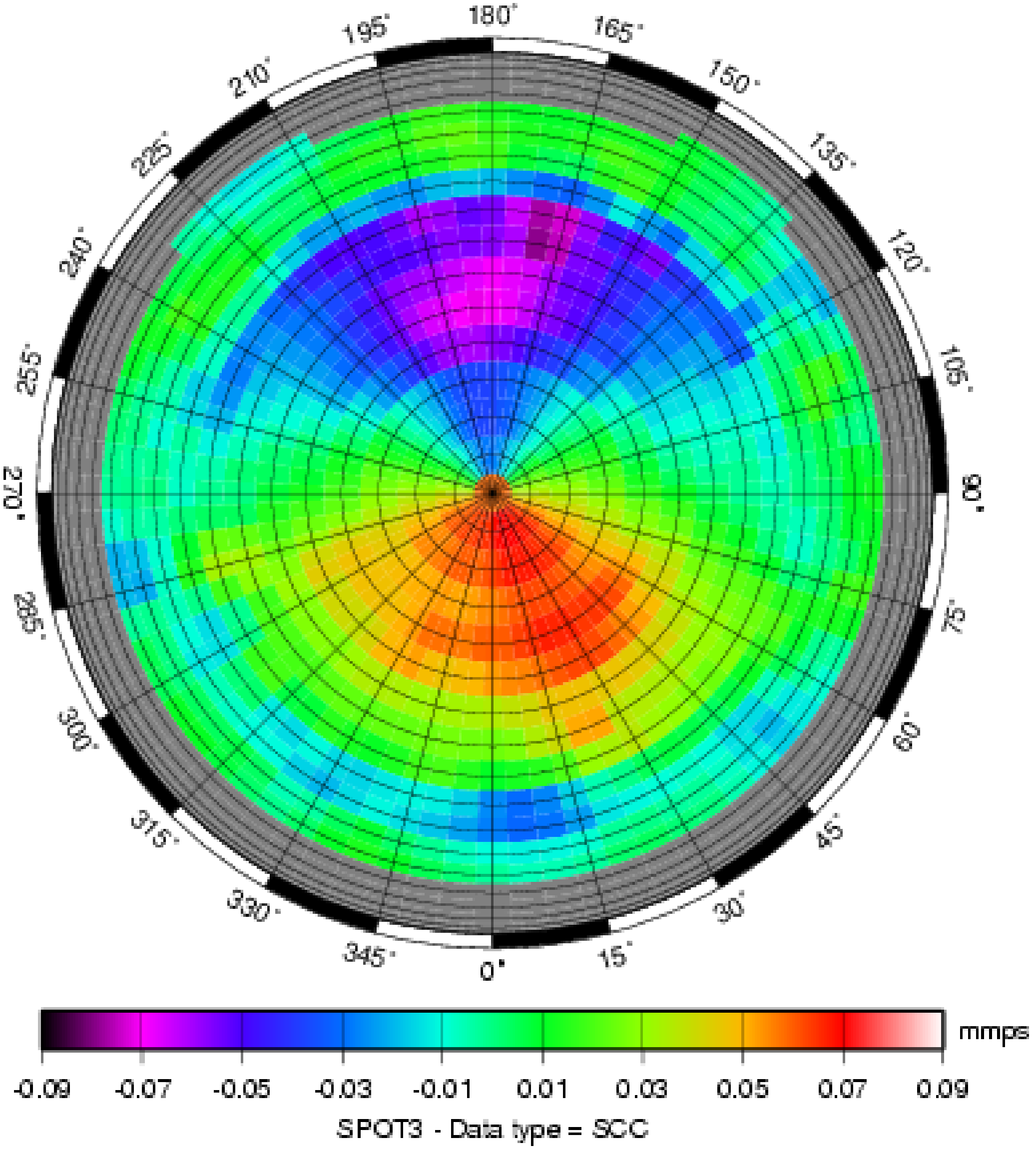

180°
165°
150°
135°
120°
105°
90°
75°
60°
45°
30°
15°
0°
345°
330°
315°
300°
285°
270°
255°
240°
225°
210°
195°
mmps
-0.09
-0.07
-0.05
-0.03
-0.01
0.01
0.03
0.05
0.07
0.09
SPOT3 - Data type = SCC

SPOT3 1996

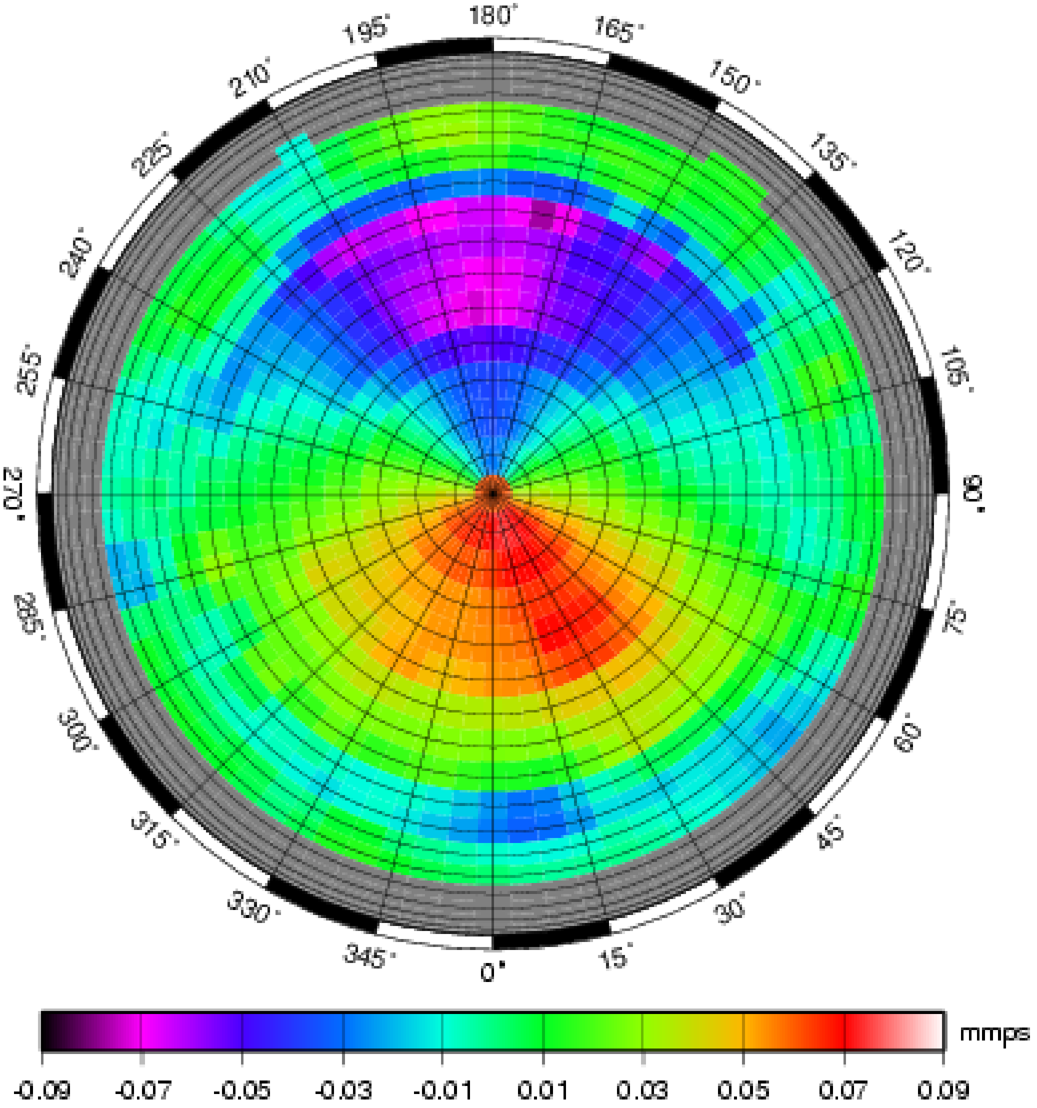

SPOT3 - Data type = SCC

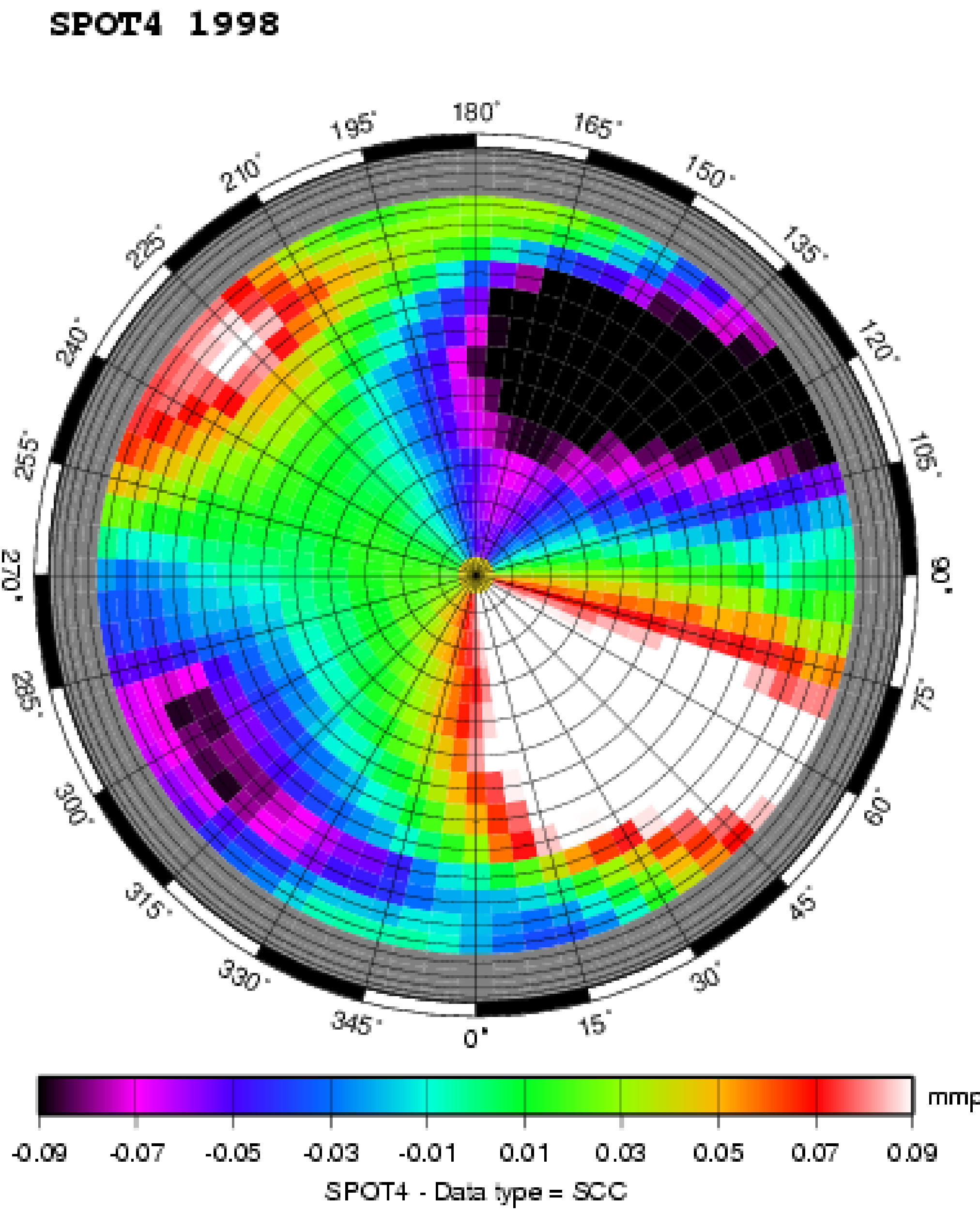
SPOT4 1998
180°
195°
165°
210°
150°
225°
135°
240°
120°
255°
105°
270°
90°
285°
75°
300°
60°
315°
45°
330°
30°
345°
15°
0°
mmps
-0.09
-0.07
-0.05
-0.03
-0.01
0.01
0.03
0.05
0.07
0.09
SPOT4 - Data type = SCC

SPOT4 2002

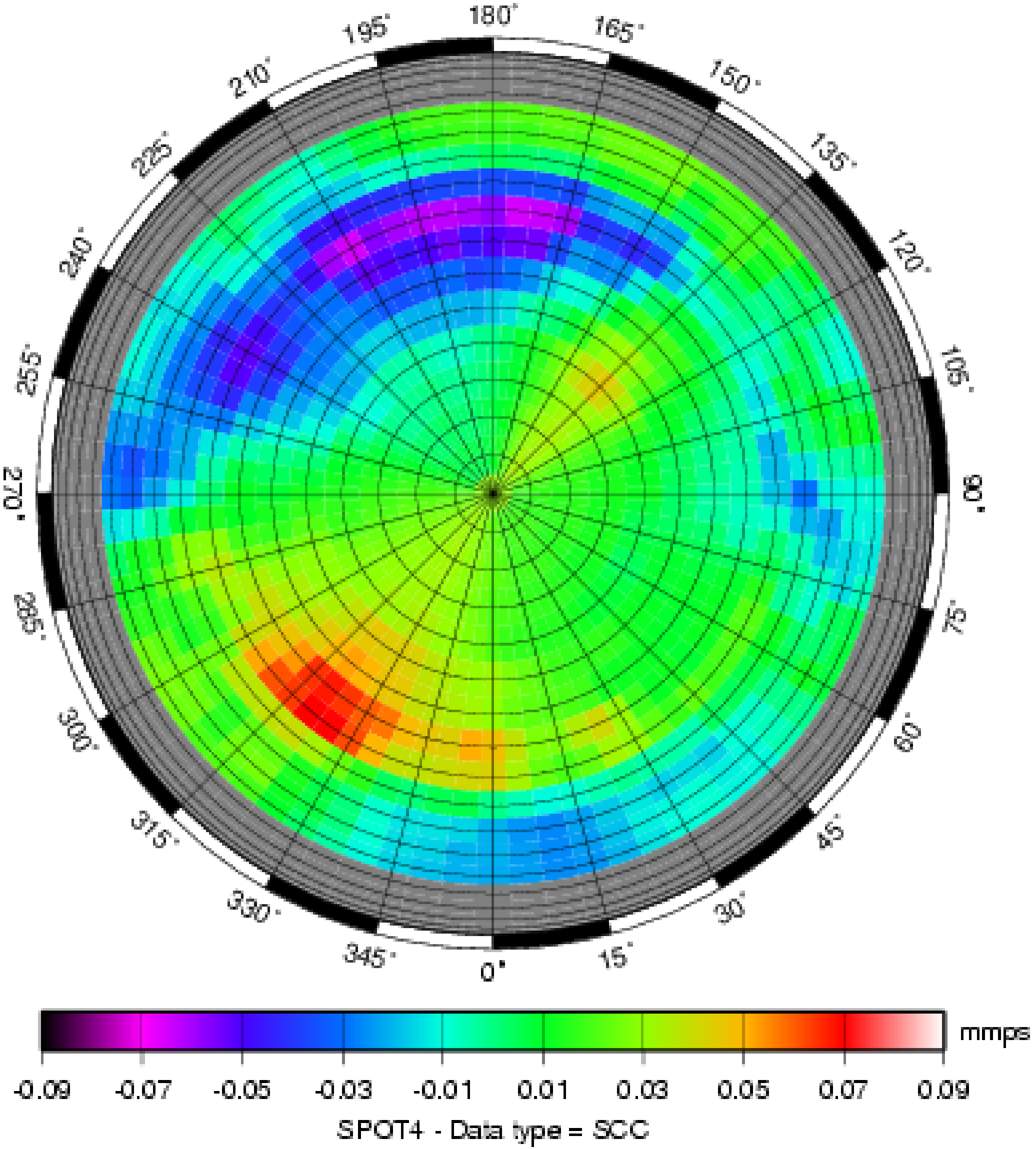

180°
195°
165°
210°
150°
225°
135°
240°
120°
255°
105°
270°
90°
285°
75°
300°
60°
315°
45°
330°
30°
345°
15°
0°
mmps
-0.09
-0.07
-0.05
-0.03
-0.01
0.01
0.03
0.05
0.07
0.09
SPOT4 - Data type = SCC

SPOT4 2003

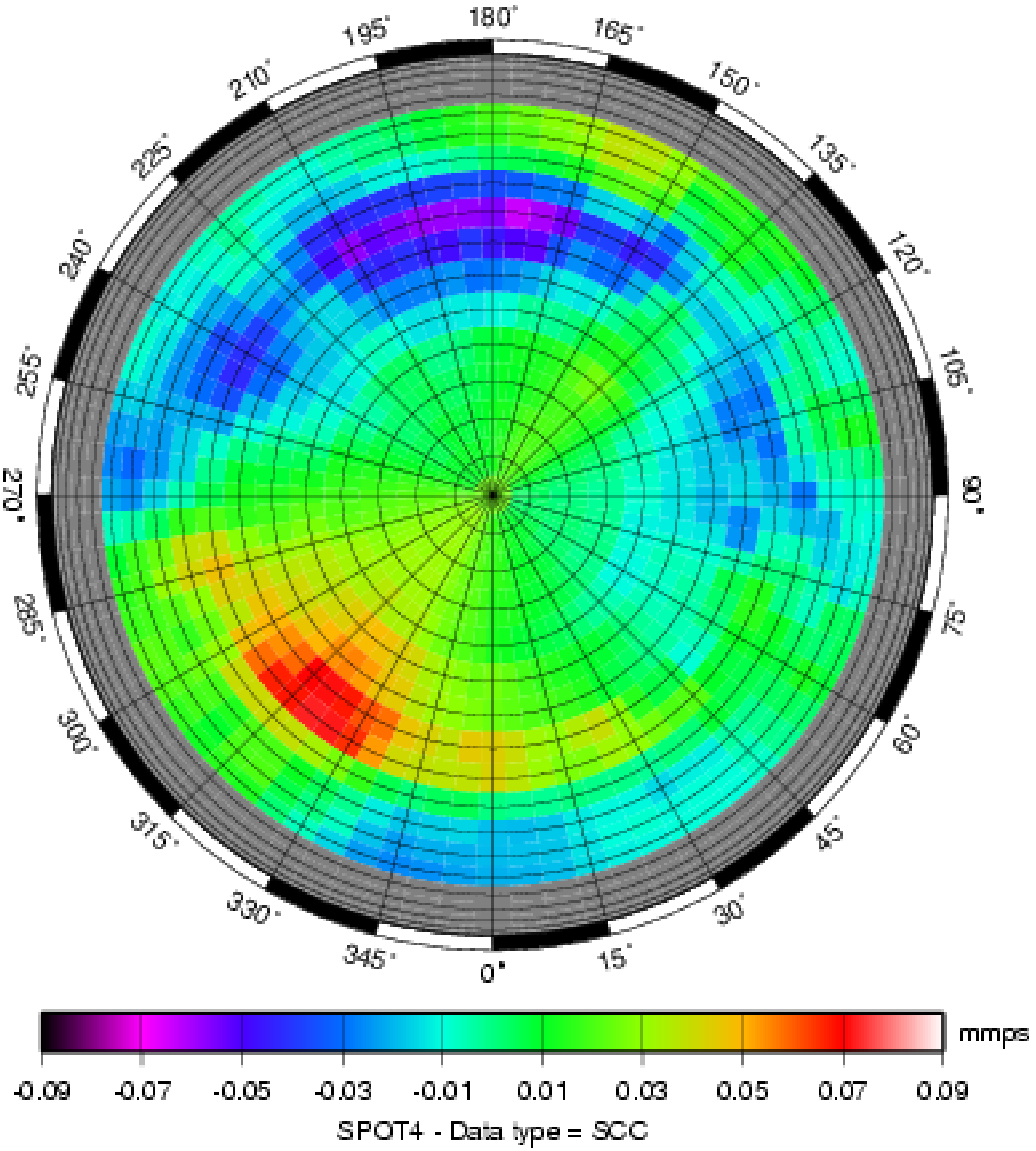
180°
195°
165°
210°
150°
225°
135°
240°
120°
255°
105°
270°
90°
285°
75°
300°
60°
315°
45°
330°
30°
345°
15°
0°
mmps
-0.09
-0.07
-0.05
-0.03
-0.01
0.01
0.03
0.05
0.07
0.09
SPOT4 - Data type = SCC

SPOT5 2002

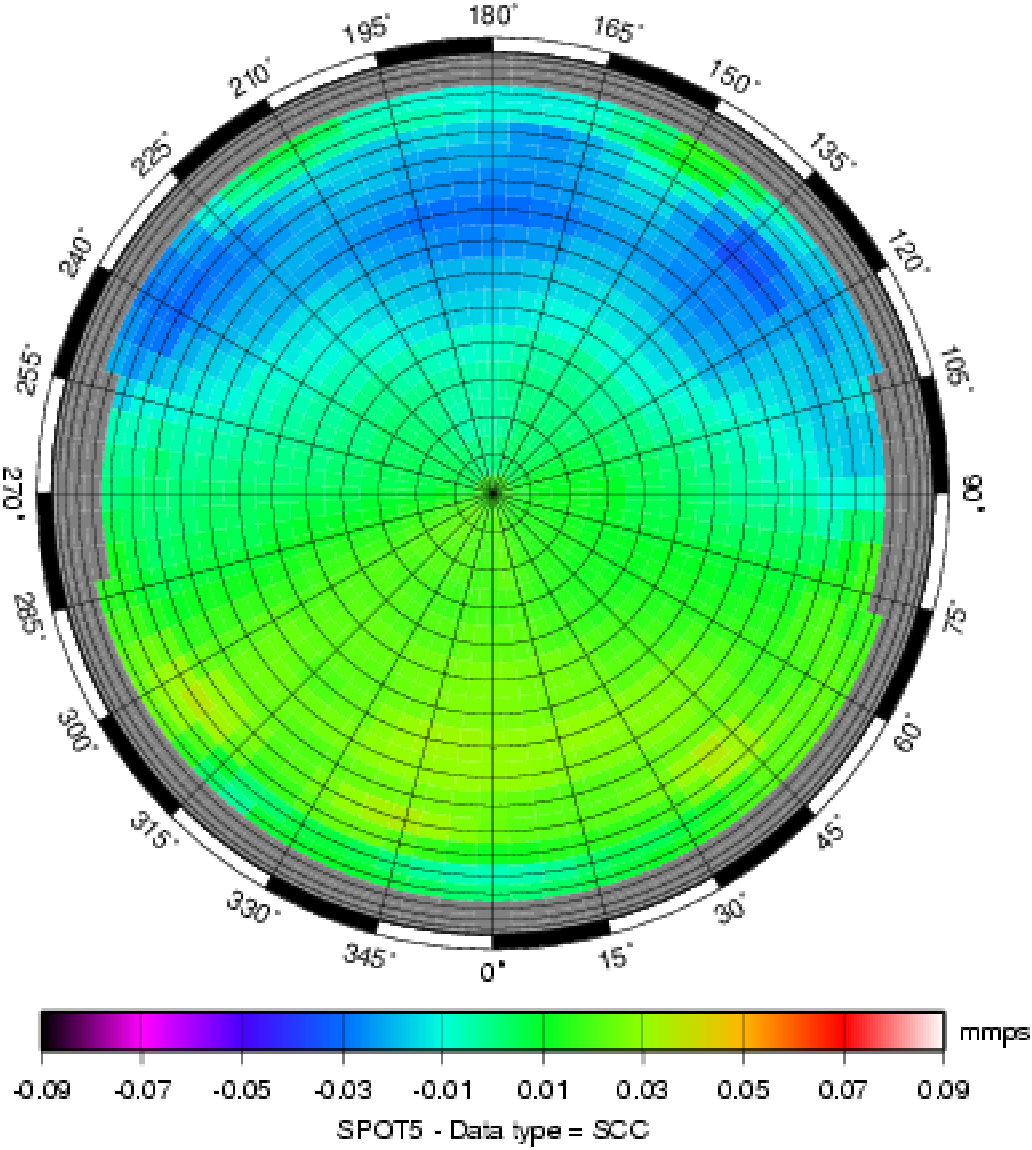

180°
195°
165°
210°
150°
225°
135°
240°
120°
255°
105°
270°
90°
285°
75°
300°
60°
315°
45°
330°
30°
345°
0°
15°
mmps
-0.09
-0.07
-0.05
-0.03
-0.01
0.01
0.03
0.05
0.07
0.09
SPOT5 - Data type = SCC

SPOT5 2003

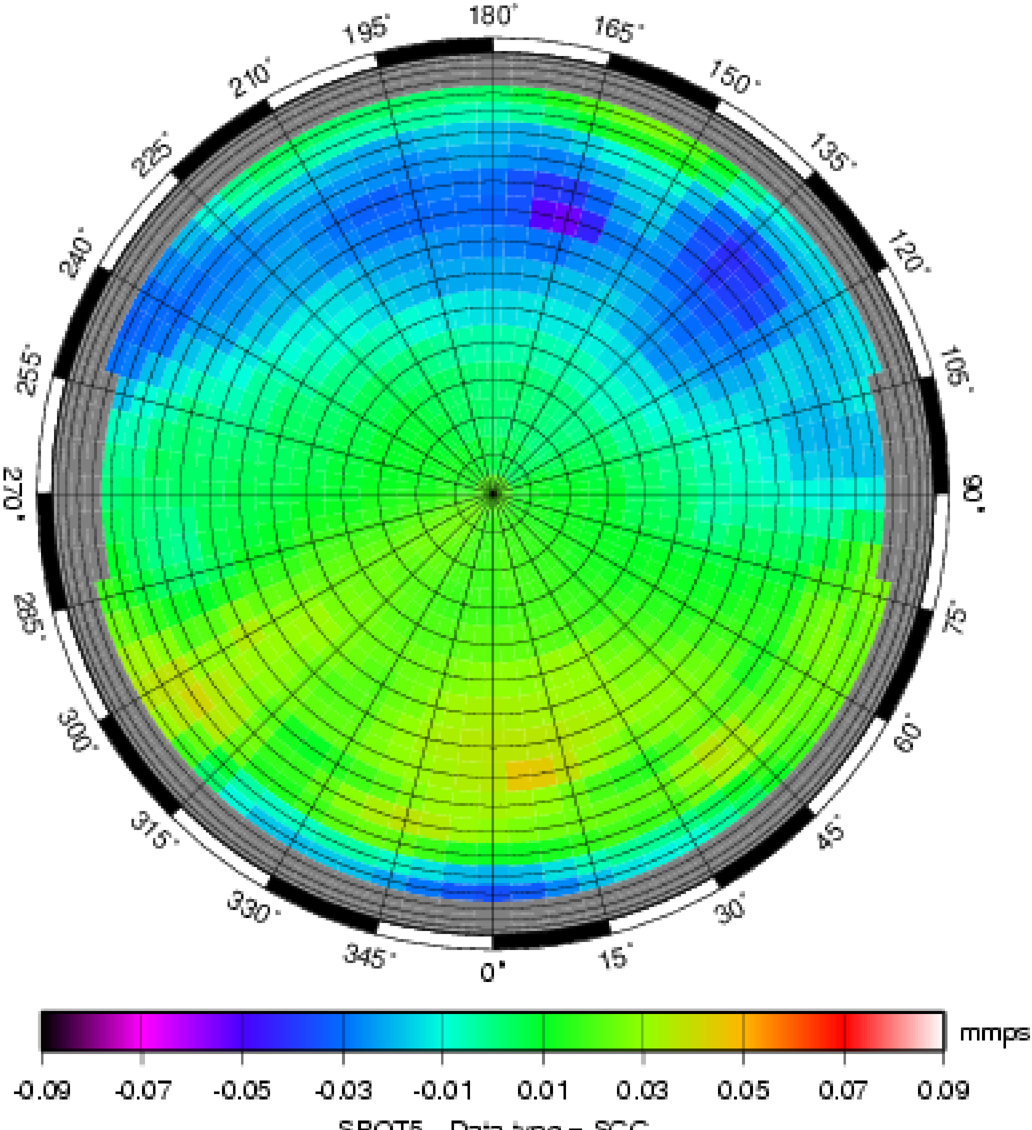

SPOT5 - Data type = SCC

TOPEX 2002

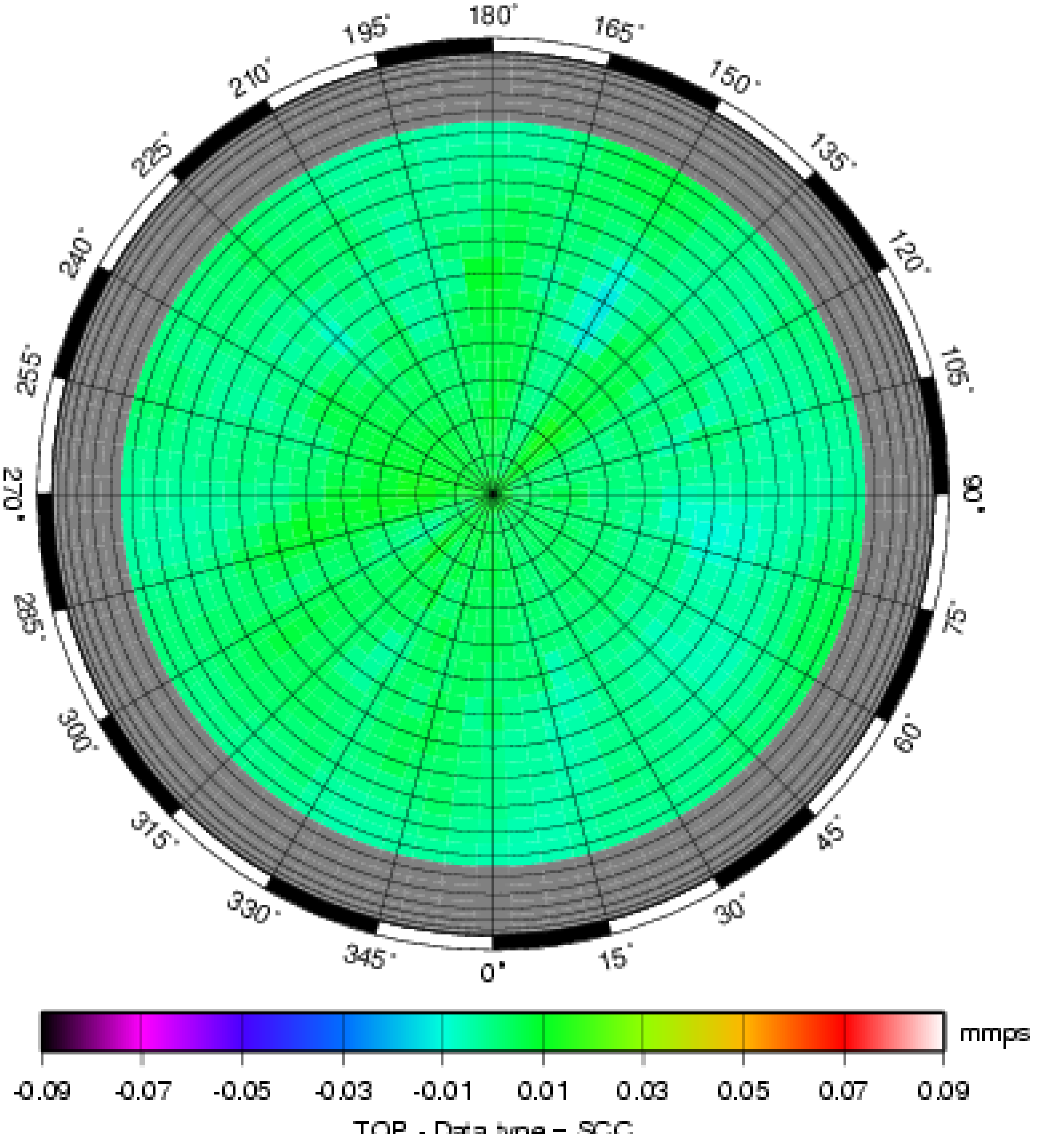

180°
195°
165°
210°
150°
225°
135°
240°
120°
255°
105°
270°
90°
285°
75°
300°
60°
315°
45°
330°
30°
345°
15°
0°
mmps
-0.09
-0.07
-0.05
-0.03
-0.01
0.01
0.03
0.05
0.07
0.09
TOP - Data type = SCC

TOPEX 2003

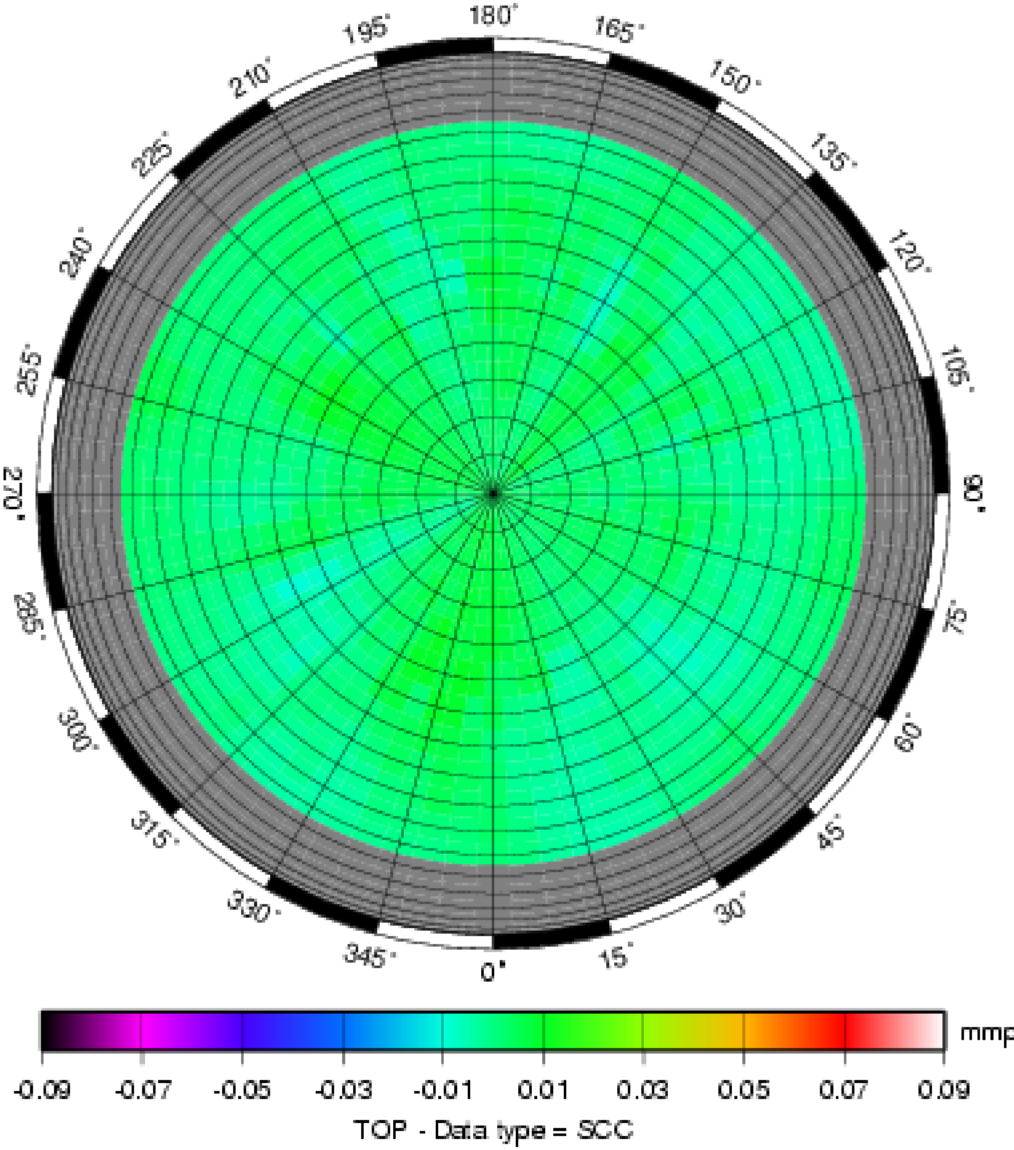
180°
195°
165°
210°
150°
225°
135°
240°
120°
255°
105°
270°
90°
285°
75°
300°
60°
315°
45°
330°
30°
345°
0°
15°
mmps
-0.09
-0.07
-0.05
-0.03
-0.01
0.01
0.03
0.05
0.07
0.09
TOP - Data type = SCC

JASON 2002

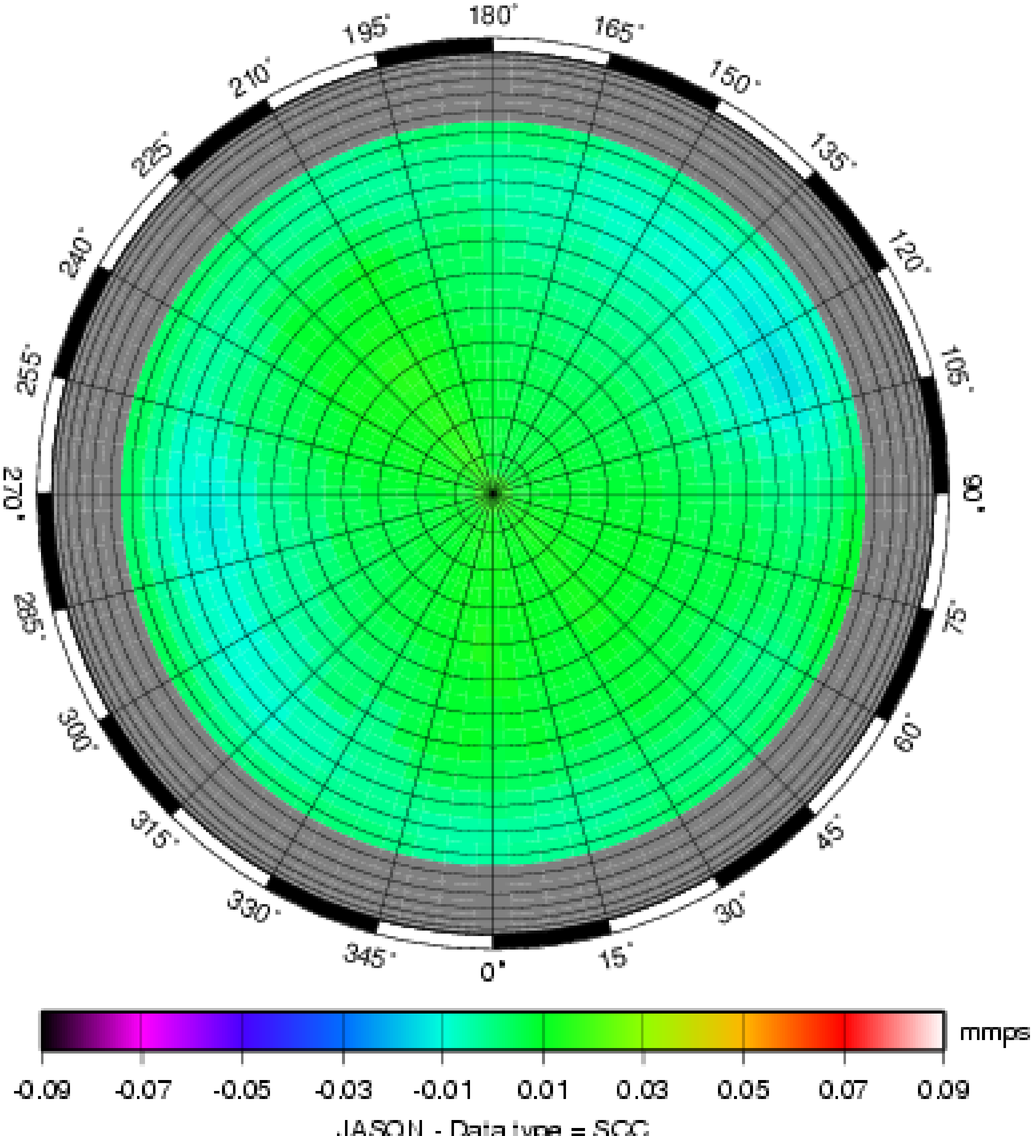
180°
195°
165°
210°
150°
225°
135°
240°
120°
255°
105°
270°
90°
285°
75°
300°
60°
315°
45°
330°
30°
345°
15°
0°
mmps
-0.09
-0.07
-0.05
-0.03
-0.01
0.01
0.03
0.05
0.07
0.09
JASON - Data type = SCC

ENVISAT 2002

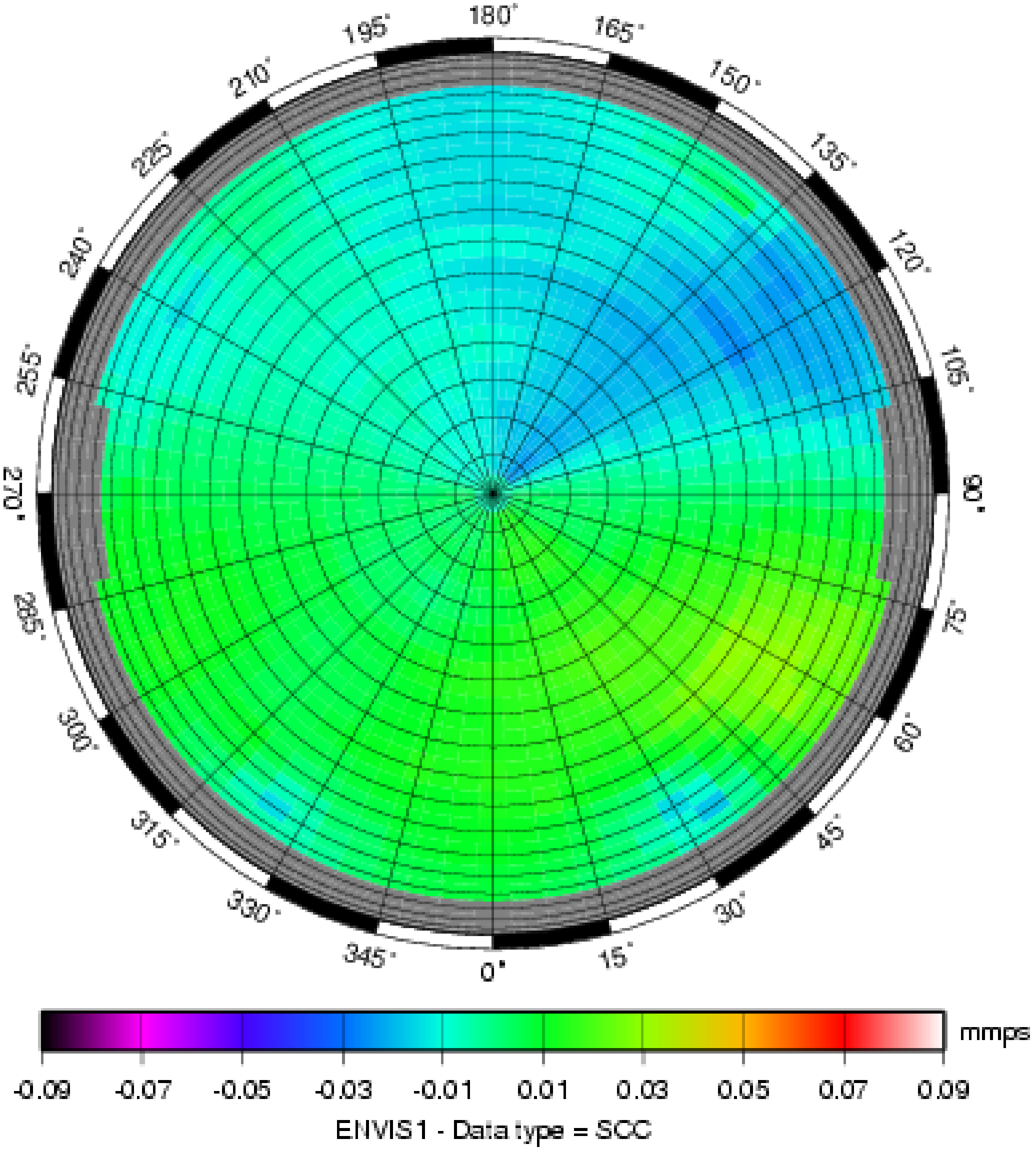

ENVISAT 2003

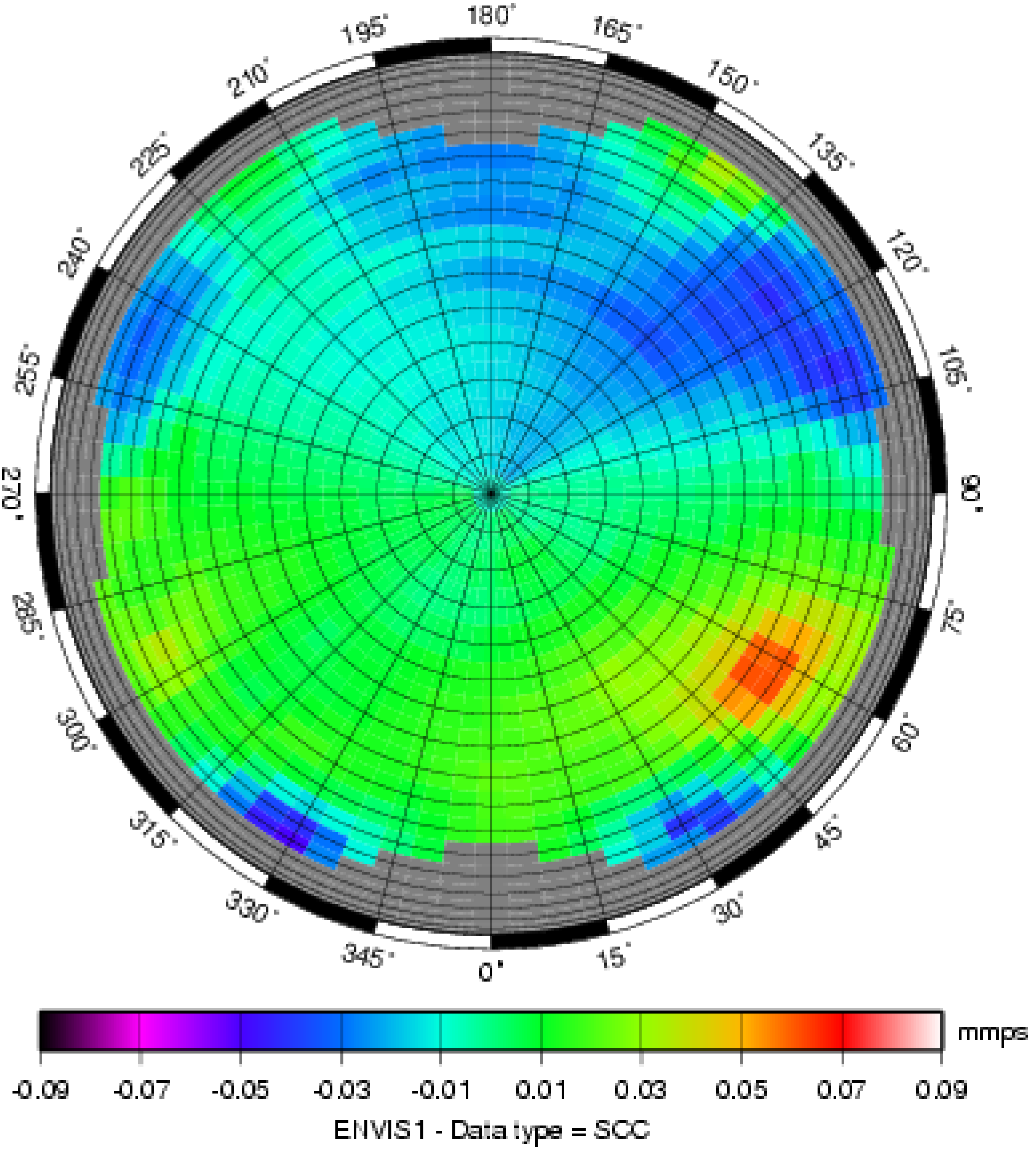

Figure 13: DORIS TOPEX/Poseidon antenna map derived from 2002 data

Figure 14: DORIS TOPEX/Poseidon antenna map derived from 2003 data

Figure 15: DORIS Jason-1 antenna map derived from 2002 data

Figure 16: DORIS Jason-1 antenna map derived from 2003 data

Figure 17: DORIS ENVISAT antenna map derived from 2002 data

Figure 18: DORIS ENVISAT antenna map derived from 2003 data

Manuscript: PSD1-B2.1-0041-04

COSPAR04-A-00083

Email contact: Pascal.Willis@ign.fr

Manuscript received: revised:
accepted: